Chemical Science

EDGE ARTICLE

View Article Online
View Journal

Cite this: DOI: 10.1039/d5sc08431h

All publication charges for this article have been paid for by the Royal Society of Chemistry

Received 31st October 2025
Accepted 14th December 2025

DOI: 10.1039/d5sc08431h

rsc.li/chemical-science

Stereodivergent access to α- and β-azanucleosides *via* catalyst-free, achiral modulator-controlled iodocyclization: a concise synthesis of forodesine

Yangyang Zhong,†[a] Jie Zeng,†[c] Mingwei Li,[a] Yuli Liang,[c] Shuman Guan,[a] Kehan Zhao,[a] Jiayi Mu,[a] Pei Tang,[a] Huijing Wang*[a] and Fener Chen *[abde]

Stereoselective glycosidic bond formation remains a major challenge in nucleoside synthesis. Azanucleosides, a prominent class of nucleoside analogs wherein the sugar oxygen is replaced by nitrogen, exhibit unique biological activities but struggle to achieve anomeric selectivity in synthesis. We disclose a catalyst-free iodocyclization strategy that uses simple achiral molecules—NaI or 2-mercaptobenzimidazole—to stereodivergently access both α- and β-azanucleosides in high yields (up to 98%) with excellent stereocontrol ($\beta:\alpha$ up to β only and $\alpha:\beta$ up to 19 : 1). The utility of this method is demonstrated by a concise synthesis of forodesine in 8 steps with 20% overall yield and >20 : 1 $\beta:\alpha$ selectivity—the shortest route and highest stereoselectivity reported to date. DFT studies reveal that hydrogen bonding/Na–O coordination and π–π stacking interactions govern the stereochemical outcomes. This work provides an efficient, scalable platform for accessing diverse azanucleoside therapeutics.

Introduction

Nucleoside analogues (NAs) are an important source of antiviral, antitumor and antibacterial drugs.[1–5] Among them, azanucleosides constitute a prominent group of structurally modified nucleosides, featuring a nitrogen-containing ring. Interestingly, β-azanucleosides usually exhibit unique physical, chemical, and biological properties.[6–8] For example, forodesine (BCX-1777, immucillin H) and galidesivir (BCX-4430, immucillin A), two well-known β-azanucleosides, are potent inhibitors of human purine nucleoside phosphorylase, protozoan nucleoside hydrolases, and purine phosphoribosyl transferases (Fig. 1).[9–12] Forodesine has been approved in Japan for the treatment of relapsed or refractory peripheral T-cell lymphoma. Galidesivir demonstrates broad-spectrum antiviral activity by disrupting viral RNA-dependent RNA polymerase.[13–20] Additionally, several other bioactive molecules structurally similar to forodesine also exhibit significant antiviral activity.[21–23] On the other hand, α-nucleosides usually have remarkable biological activities, high enzyme stabilities, and inhibitory activities against tumors, bacteria, and plasmodia.[24] However, investigations of α-azanucleosides are merely at the initial stage, due to limited synthetic methods. Given the importance of both β- and α-azanucleosides, it is essential to develop a stereocontrolled synthetic strategy applicable to both configurations.

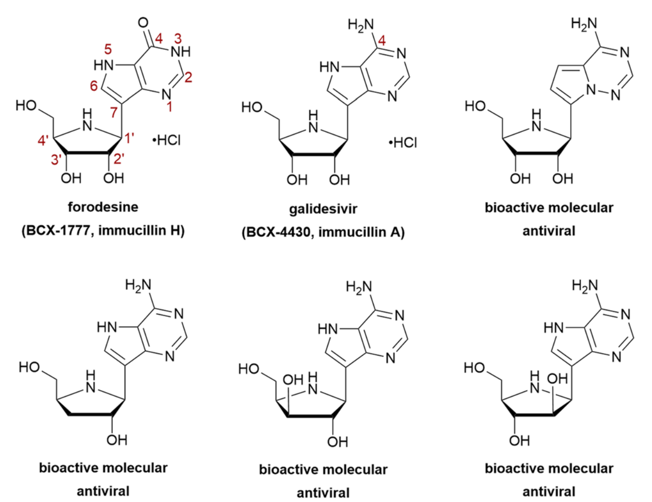

Fig. 1 Structures of representative azanucleoside drugs and bioactive molecules.

[a]Sichuan Research Center for Drug Precision Industrial Technology, West China School of Pharmacy, Sichuan University, Chengdu, 610041, China. E-mail: wanghuijing@scu.edu.cn; rfchen@fudan.edu.cn

[b]Institute of Flow Chemistry and Engineering, College of Chemistry and Materials, Jiangxi Normal University, Nanchang, Jiangxi, 330022, China

[c]Pharmaceutical Research Institute, Wuhan Institute of Technology, 430205, Wuhan, China

[d]Engineering Center of Catalysis and Synthesis for Chiral Molecules, Department of Chemistry, Fudan University, Shanghai Engineering Center of Industrial, Shanghai, 200433, China

[e]Asymmetric Catalysis for Chiral Drugs, Shanghai 200433, China

† These authors contributed equally to this work.

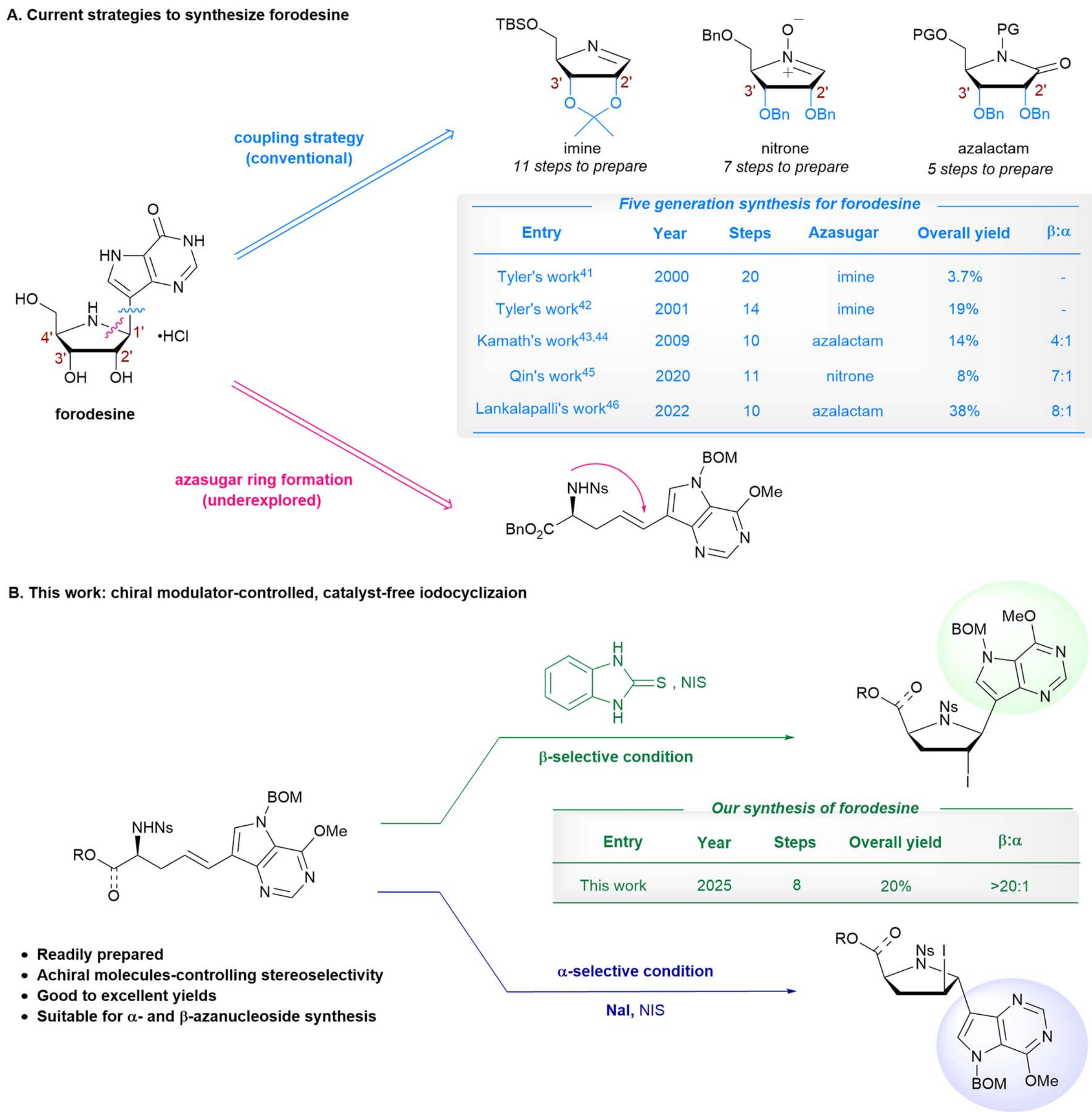

Fig. 2 (A) Current strategies to synthesize forodesine. (B) This work: catalyst-free, achiral modulator-controlled iodocyclization for stereoselective synthesis of α- and β-azanucleosides.

C-Glycosylation is the most widely used method for synthesizing *C*-nucleosides, including eletrophillic addition,[25] nucleophilic addition,[26–29] the Friedel–Crafts reaction,[30,31] metal cross coupling,[32–35] and radical-mediated reactions.[36–40] Current strategies for synthesizing β-azanucleosides, as exemplified by the synthesis of forodesine, primarily involve constructing the key glycosidic bond through coupling reactions (Fig. 2A).[41–47] To achieve milder reaction conditions, improved stereoselectivity and higher yields, various sugar donors have been developed, such as imines, nitrones, and azalactams. Among all reported synthetic routes to forodesine, the highest $\beta : \alpha$ selectivity is 8 : 1, with a maximum yield of 38%.[47] The synthesis of galidesivir follows a similar strategy, focusing mainly on introducing the amine group at the C4 position of the purine ring.[45] Nevertheless, existing intermolecular cross-coupling methods for β-azanucleosides face two major challenges: (1) the synthesis of azasugar donors is often complex, typically requiring at least five steps from furanose with low efficiency; (2) control over glycosidic bond stereoselectivity remains unsatisfactory and is highly dependent on auxiliary groups at the C2′ position of the glycosyl donor.

Catalytic asymmetric halocyclization of alkenes has proven to be a powerful strategy for accessing stereodefined heterocycles while installing halogen handles for further functionalization.[48–51] In our previous work, we established a chiral phosphoric acid-catalyzed intramolecular iodocyclization system for the synthesis of furanose nucleosides, in which achiral additives (NaI or S=PPh_3) were employed to modulate anomeric stereoselectivity.[52] However, this system suffered from two critical limitations: it proved ineffective for synthesizing azanucleosides where the nucleophile is an

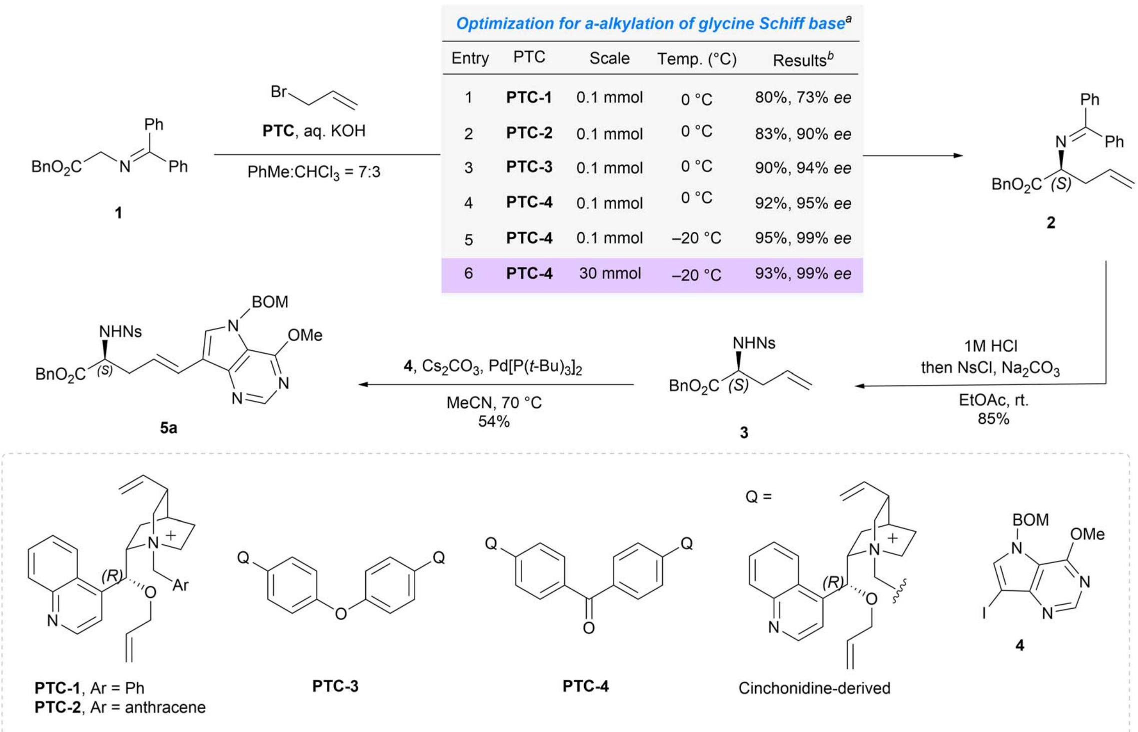

Optimization for a-alkylation of glycine Schiff base[a]

Entry	PTC	Scale	Temp. (°C)	Results[b]
1	**PTC-1**	0.1 mmol	0 °C	80%, 73% *ee*
2	**PTC-2**	0.1 mmol	0 °C	83%, 90% *ee*
3	**PTC-3**	0.1 mmol	0 °C	90%, 94% *ee*
4	**PTC-4**	0.1 mmol	0 °C	92%, 95% *ee*
5	**PTC-4**	0.1 mmol	–20 °C	95%, 99% *ee*
6	**PTC-4**	30 mmol	–20 °C	93%, 99% *ee*

Scheme 1 The synthesis of compound **5a**. [a]Reaction conditions: 1 (0.1 mmol), allyl bromide (0.12 mmol), **PTC** (0.0005 mmol), 50% aq. KOH (0.25 mL) in PhMe : $CHCl_3$ ($v:v = 7:3$, 0.75 mL), 0 °C, 8 h. [b]Isolated yield, ee values were determined by chiral HPLC.

NHR group, failing to deliver either α- or β-configured products with satisfactory stereocontrol (see SI Table S1); moreover, its reliance on a chiral phosphoric acid catalyst severely limited practicality and scalability. Indeed, industrial adoption of chiral phosphoric acid catalysts is often hampered by the high cost associated with the six-step synthesis from BINOL. The global environmental factor (E_G factor) highlights environmental drawbacks in synthetic systems by quantifying waste generation across the full lifecycle, including catalyst synthesis and reaction processes.[53,54] Reducing the use of expensive chiral catalysts represents a straightforward approach to minimize the E_G factor.

To address these challenges, we have developed a fundamentally distinct, catalyst-free iodocyclization strategy. Stereodivergent synthesis of azanucleosides is achieved in the absence of any chiral catalyst, using only simple achiral modulators: NaI for α-selectivity and 2-mercaptobenzimidazole for β-selectivity (Fig. 2B). This approach not only avoids the cost and environmental burden associated with chiral catalysts but also successfully addresses the long-standing challenge of stereoselective azanucleoside formation. The resulting C2-iodinated products serve as versatile intermediates for further functionalization, enabling efficient access to both α- and β-azanucleosides, including a concise synthesis of forodesine. We believe that this method provides a robust and scalable platform for diversifying azanucleosides, which remain underexplored in medicinal chemistry.

Results and discussion

Our synthesis commenced with the preparation of halocyclization substrate **5a** (Scheme 1). Asymmetric α-alkylation of glycine Schiff base catalyzed by chiral phase-transfer catalysts (**PTC**) is a well-established method for accessing unnatural amino acids.[55–61] Quinuclidinium salts, derived from cinchonidine and cinchonine, are widely used to induce stereoselectivity.[62–65] To enhance the enantioselectivity, we chose glycine Schiff base **1** bearing a benzyl ester group instead of the conventional *tert*–butyl ester. The performance of cinchonidine-derived quinuclidinium salts (**PTC-1 to 4**) in the enantioselective allylation of **1** was evaluated (entries 1–4). The dimeric cinchonidine derivative linked by a benzophenone group (**PTC-4**) proved highly effective, affording product **2** with excellent enantioselectivity (entry 4, 92% yield, 95% ee). Lowering the reaction temperature improved both reactivity and enantioselectivity, giving **2** in 95% yield and 99% ee (entry 5). This condition performed well even on a 30 mmol scale (entry 6, 93% isolated yield, 99% ee). Acid deprotection afforded the free amine intermediate, which was subsequently protected with an Ns (nitrobenzenesulfonyl) group to yield compound **3** in 85% yield. A Heck reaction between aryl iodine **4** and alkene **3** in the presence of Pd[P(t-Bu)$_3$]$_2$ and Cs_2CO_3 furnished the C–C coupling product **5a**, which served as the substrate for subsequent halocyclization.

In our previous work, NaI and S═PPh_3 were identified as key additives for controlling the stereoselectivity of catalytic

Table 1 Optimization of reaction conditions[a]

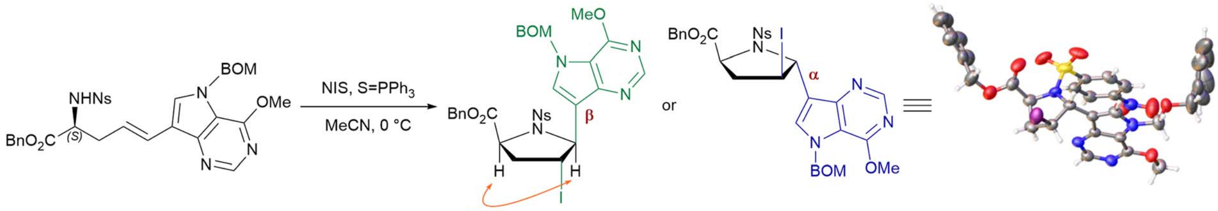

5a 6a 7a

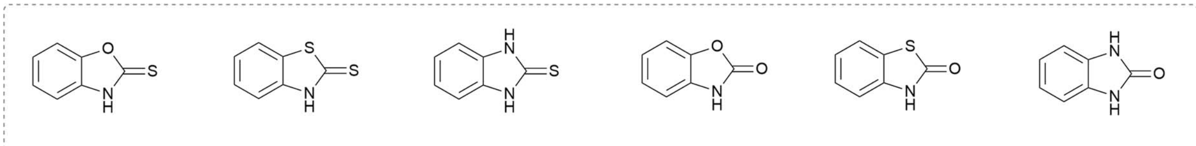

8 9 10 11 12 13

Entry	Variation from labeled conditions	Yield[b] (%)	$\beta:\alpha$ (**6a** : **7a**)[c]
1	None	92	5 : 1
2	No S=PPh$_3$	95	1 : 1
3	NaI instead of S=PPh$_3$	85	1 : 10
4	**8** instead of S=PPh$_3$	93	11 : 1
5	**9** instead of S=PPh$_3$	95	10 : 1
6	**10 instead of S=PPh$_3$**	**95**	**25 : 1**
7	**11** instead of S=PPh$_3$	80	2 : 1
8	**12** instead of S=PPh$_3$	82	5 : 1
9	**13** instead of S=PPh$_3$	79	2 : 1
10	**NaI instead of S=PPh$_3$, THF instead of MeCN**	**93**	**1 : 19**
11	No S=PPh$_3$, THF instead of MeCN	90	1 : 3

[a] Reaction conditions: **5a** (0.05 mmol), NIS (0.10 mmol), S=PPh$_3$ (0.05 mmol) in MeCN (2.5 mL), 0 °C for 1 h. [b] Isolated yield. [c] $\beta:\alpha$ values were determined by HPLC.

halocyclization by directing the reaction along specific pathways.[52] Therefore, we first investigated the effect of S=PPh$_3$ on stereochemical control (Table 1). Pleasingly, when S=PPh$_3$ was used as an achiral modulator with NIS as the halogen source, β-nucleoside **6a** was obtained as the major product (entry 1; $\beta:\alpha = 5:1$). In contrast, when NaI was used as the modulator, the configuration inverted, affording α-nucleoside **7a** with a $\beta:\alpha$ ratio of 1 : 10 (entry 3). The absolute configuration of **7a** was confirmed by single-crystal X-ray crystallography (CCDC No. 2378539). The configuration of **6a** was then assigned by comparing its NMR NOE (Nuclear Overhauser Effect) data with those of **7a.** In the absence of any modulator, no stereocontrol was observed (entry 2). These results suggested that the thiocarbonyl group might be crucial for β-selectivity. We then screened various thiocarbonyl-containing compounds as β-selective modulators (see SI Table S2). Among them, 2-mercaptobenzoheterocycles exhibited excellent reactivities and stereoselectivities (entries 4–6). Notably, 2-mercaptobenzimidazole **10** afforded product **6a** in high yield (up to 95%) with excellent β-selectivity ($\beta:\alpha = 25:1$; entry 6). To verify the necessity of the thiocarbonyl group, control experiments with compounds **11**, **12**, and **13** were conducted (entries 7–9). These compounds showed almost no stereocontrol. We further optimized the reaction conditions to improve α-selectivity (see SI Table S3). By fine-tuning the solvent, high α-selectivity was achieved ($\beta:\alpha = 1:19$, entry 10). In the absence of NaI, the diastereomeric ratio was only $\beta:\alpha = 1:3$ (entry 11). Loading studies revealed that both NaI and **10** could promote stereoselective iodocyclization catalytically. High α-selectivity was maintained ($\beta:\alpha = 1:19$), while β-selectivity slightly decreased ($\beta:\alpha = 1:14$) under reduced loading of **10** (see SI Table S4).

We systematically evaluated the substrate scope under both β- and α-selective conditions, using a series of halocyclization substrates **5a–u** bearing varied R^1 groups and nucleobase structures (Fig. 3). Starting from model substrate **5a**, the effect of different ester groups (R^1=CO$_2$Me, CO$_2$*t*-Bu) was examined. Both β-azanucleosides **6b–c** and α-azanucleosides **7b–c** were obtained in high yields (>90%) with excellent stereoselectivity ($\beta:\alpha$ up to 24 : 1 and $\alpha:\beta$ up to 17 : 1). To closely mimic the azanucleoside structure, a hydroxymethyl group protected with various groups (TBS, TBDPS, MOM, and Bn) was introduced at the C4′ position. Substrates **5d–g** performed well, affording β-azanucleosides **6d–g** in high yields (>80%) with good stereocontrol ($\beta:\alpha$ up to 18 : 1) and α-azanucleosides **7d–g** in high yields (>87%) with moderate

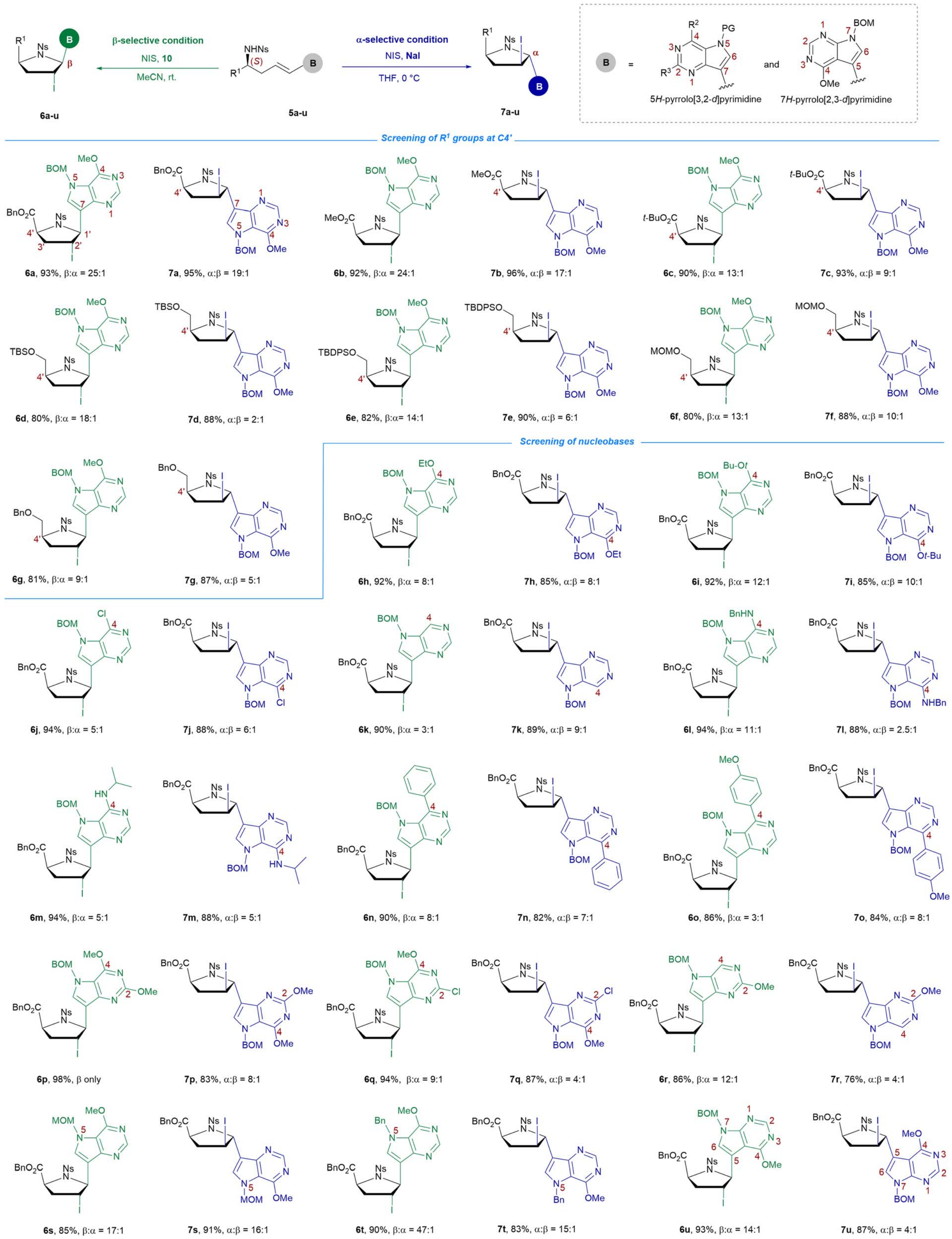

Fig. 3 Substrate scope of α- and β-azanucleoside synthesis.

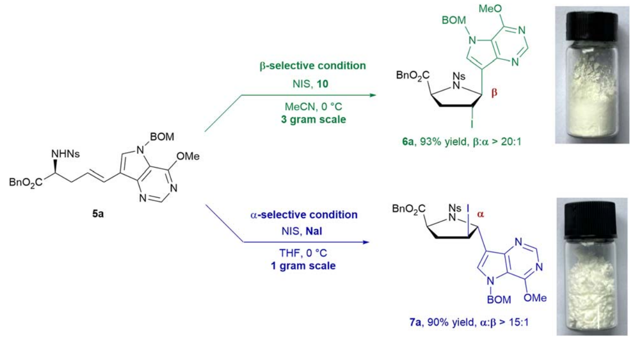

Fig. 4 Gram-scale synthesis of β-azanucleoside **6a** and α-azanucleoside **7a** *via* catalyst-free, achiral modulator-controlled iodocyclizations.

stereocontrol ($\alpha:\beta$ up to 10 : 1). In the screening of nucleobase structures, we systematically examined the influence of substituents in 5*H*-pyrrolo[3,2-*d*]pyrimidine derivatives. Both mono-substituted derivatives at the C4-position (such as OEt, O*t*Bu, Cl, H, NHBn, NH*i*-Pr, Ph, and 4-OMe-Ph) and disubstituted derivatives at the C2 and C4 positions generally exhibited good to excellent stereoselectivity under the optimized conditions. β-Azanucleosides **6h–r** were formed with high selectivity ($\beta:\alpha$ up to β only) and high yields (>86%), except for **6k** and **6o** ($\beta:\alpha = 3:1$). Similarly, α-azanucleosides **7h–r** were mostly obtained with high selectivity ($\alpha:\beta$ up to 10 : 1), except for **7l** ($\alpha:\beta = 2.5:1$). Evaluation of N5-protecting groups (such as MOM and Bn) showed that they could direct the formation of the corresponding β-azanucleosides **6s–t** and α-azanucleosides **7s–t** with excellent stereoselectivities. Finally, preliminary evaluation of the 7*H*-pyrrolo[2,3-*d*]pyrimidine scaffold confirmed the good compatibility of the reaction system.

To demonstrate scalability, β-nucleoside analogue **6a** and α-nucleoside analogue **7a** were synthesized on a gram scale from **5a** (Fig. 4). Both yields and stereoselectivities were maintained: β-nucleoside **6a** was obtained in 93% yield with $\beta:\alpha > 20:1$, and α-nucleoside **7a** in 90% yield with $\alpha:\beta > 15:1$.

Using this β-selective iodocyclization as the key step, we developed an efficient asymmetric synthesis of forodesine and a formal synthesis of galidesivir. As shown in Scheme 2, forodesine was synthesized in 20% overall yield over eight steps from commercially available glycine Schiff base **1**. Starting from the β-selective iodocyclization product **6a**, one-pot reductive debenzylation and halide elimination smoothly afforded compound **14** in 75% yield. Stereospecific *syn*-dihydroxylation of **14** with OsO_4, followed by deprotection, gave compound **15**. Treatment of **15** with HCl in methanol then furnished forodesine. Following literature procedures,[45] functional group modifications of the base moiety in forodesine, followed by deprotection, provided the bioactive compound galidesivir. To the best of our knowledge, this work provides the shortest route to forodesine (8 steps *vs.* 10 in prior reports) and the highest $\beta:\alpha$ selectivity (>20 : 1 *vs.* 8 : 1).

To demonstrate the versatility of our method and its potential for constructing compound libraries in medicinal chemistry, we performed diverse derivatizations on both β- and α-azanucleosides (Scheme 3). Specifically, β-nucleoside **6a** underwent reductive elimination with $NaBH_4$/DBU, affording alkene **14** in 75% yield. Removal of the Ns group under 1-mercaptooctane/*t*-BuOK conditions gave **17** in 87%

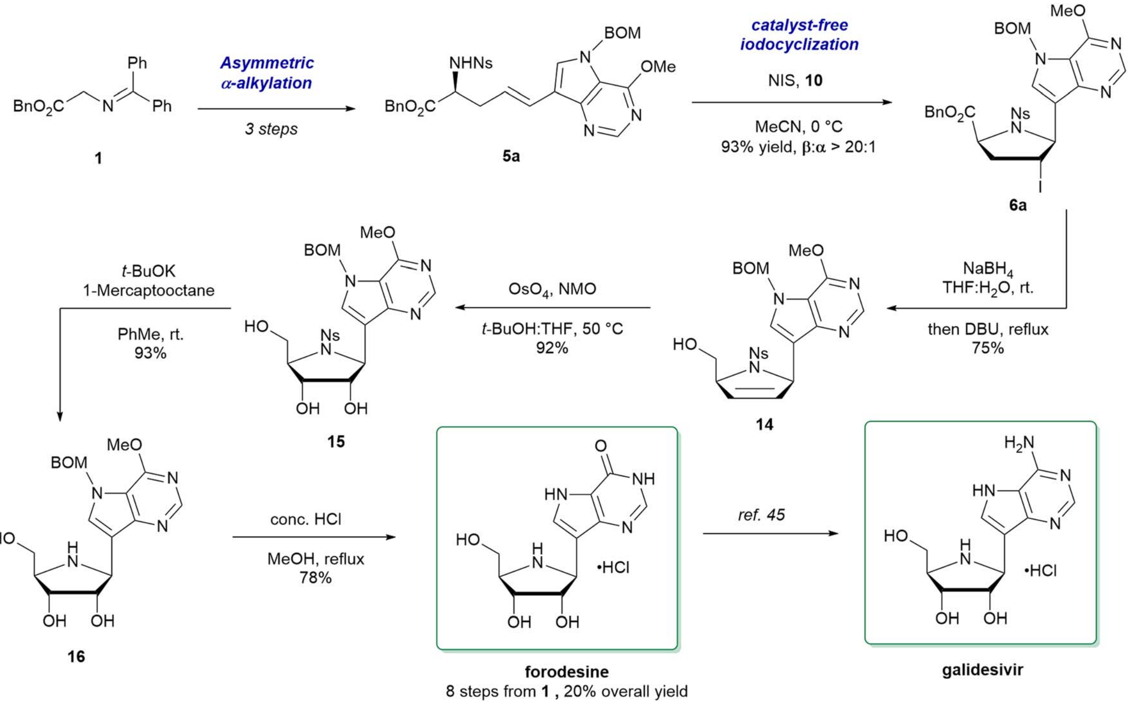

Scheme 2 Concise synthesis of forodesine and galidesivir.

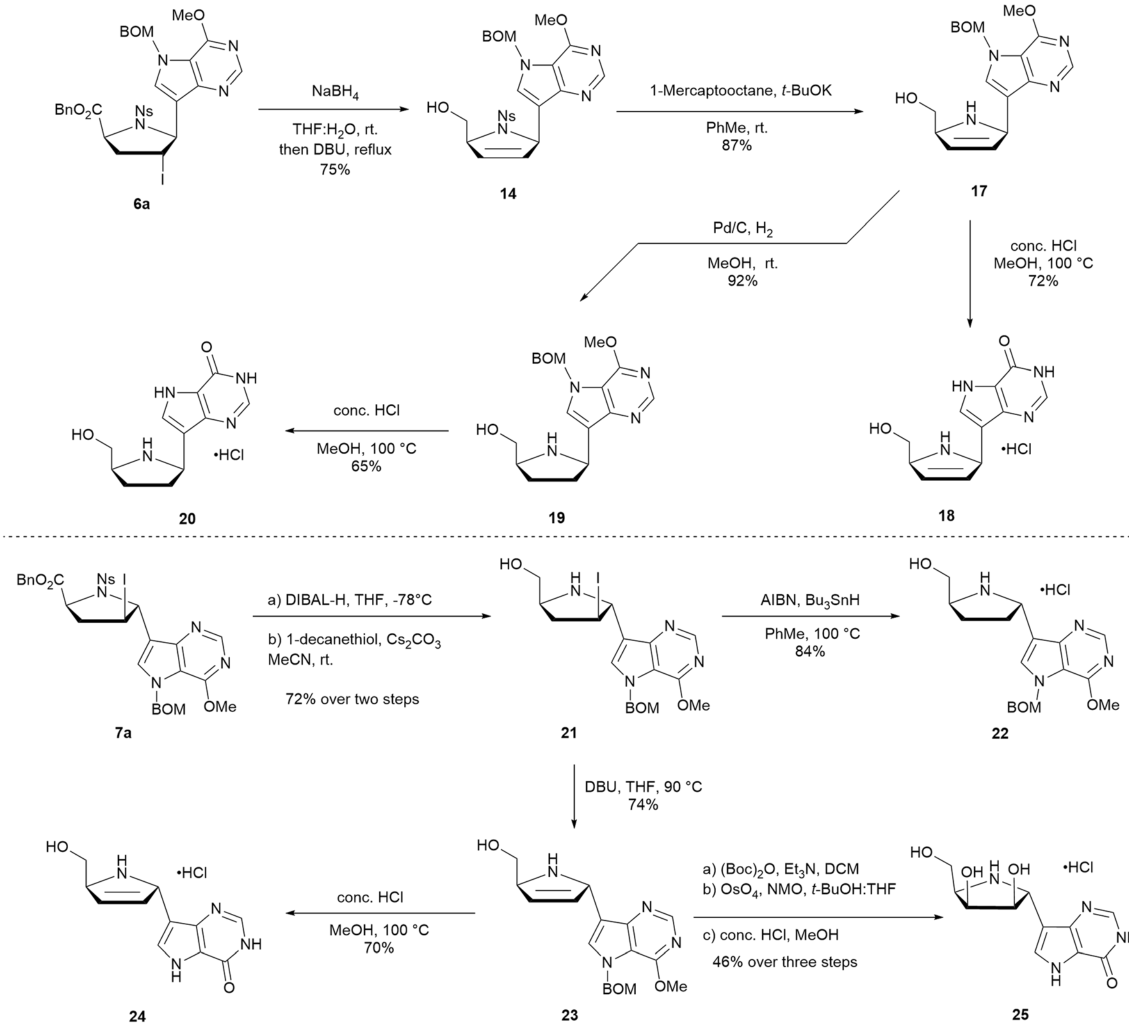

Scheme 3 Derivatization of β-azanucleoside **6a** and α-azanucleoside **7a**.

yield. Subsequent reflux of **17** in concentrated HCl/MeOH furnished **18** in 72% yield. Alternatively, hydrogenation of **17** followed by deprotection afforded the C2′ and C3′-unsubstituted azanucleoside **20** in 60% yield over two steps. For the α-azanucleoside series, treatment of **7a** with DIBAL-H and subsequent Ns deprotection provided **21** in 72% yield. Radical-mediated deiodination of **21** yielded **22**, while DBU-promoted elimination afforded alkene **23** in 74% yield. Treatment of **23** with concentrated HCl gave **24**. Furthermore, **23** served as a key intermediate for the stereoselective synthesis of target compound **25**. This was achieved *via* Boc protection of the C4′ hydroxymethyl group, dihydroxylation of the C2′–C3′ alkene (occurring exclusively from the β-face to give the corresponding diol), and final Boc deprotection.

To gain a thorough understanding of the reaction mechanism, especially on the effect of two achiral molecules, NaI and 2-mercaptobenzimidazole **10**, density functional theory (DFT) studies were performed at the PBE0 level,[66] using alkene **5a** as a model substrate (Fig. 5). The α-selective iodocyclization starts from **Int1** (-4.6 kcal mol^{-1}). We used the interaction region indicator (IRI)[67,68] to analyze the interactions between atoms of **Int1** (IRI pic. of **Int1**). Interestingly, NaI in **Int1** is identified as a centered role, cooperating with Ns and ester carbonyl oxygen through Na–O interactions. And Ns can stabilize NIS through π…π stacking, allowing NIS to attack substrates from the top face. These interactions provide a favorable spatial environment for α-selectivity. The electrophilic addition of I^- to **5a** and meanwhile H^+ being transferred to the N atom result in **Int2** with a reaction barrier of 22.5 kcal mol^{-1}. The following nucleophilic cyclization occurs to generate **PS**, which is exergonic by 25.1 kcal mol^{-1}. In the β-selective iodocyclization pathway, the IRI result of **Int3** reveals that due to the hydrogen bonding interaction, the thiol **10** consistently occupies the region above the C═C bond throughout the reaction. Due to the steric effect, the I^- from NIS attacks the alkene from the bottom face only, resulting in β-selectivity. Finally, nucleophilic cyclization is found to be exergonic by 16.9 kcal mol^{-1}, and the reaction barrier is 32.5 kcal mol^{-1} (**Int3** to **PR**).

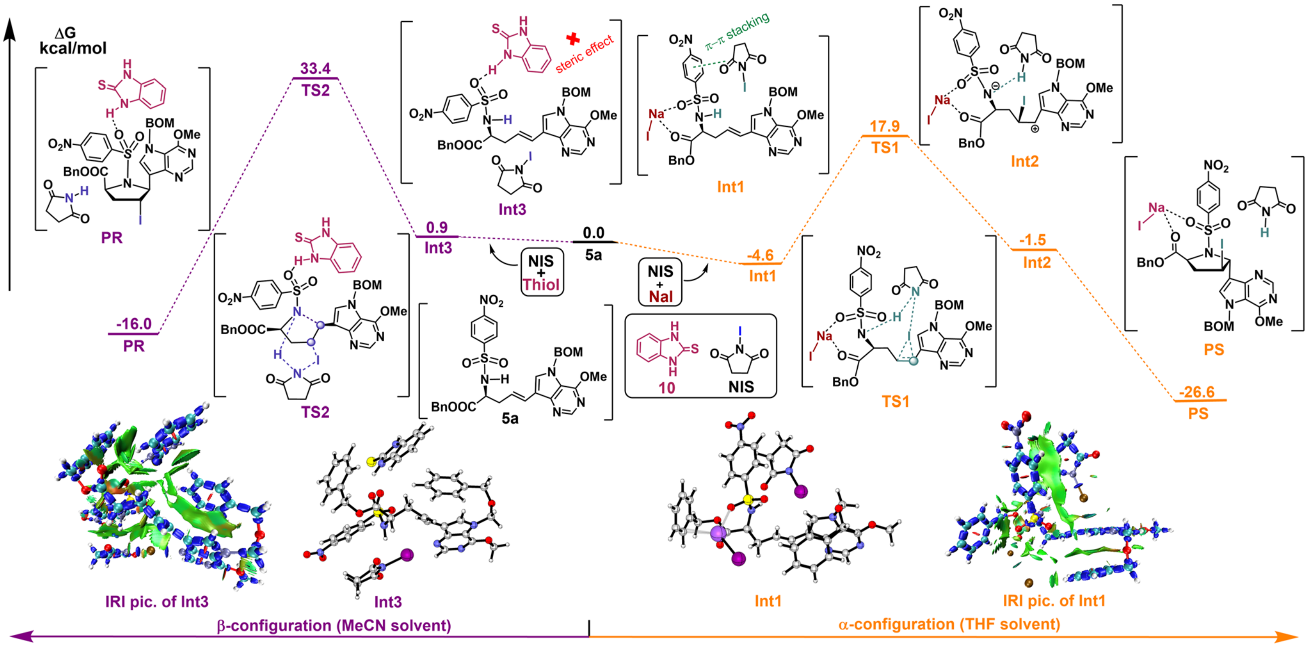

Fig. 5 Calculated free energy profile for the formation of nucleosides with α- and β-configurations from substrate **5a** and other reactants.

Conclusion

In summary, we developed a catalyst-free iodocyclization strategy using two simple achiral molecules, NaI and 2-mercaptobenzimidazole **10**, for the stereoselective synthesis of α- and β-azanucleosides in high yields and stereoselectivities. DFT studies reveal that NaI directs α-selectivity through hydrogen bonding and Na–O coordination, while 2-mercaptobenzimidazole **10** controls β-selectivity *via* π–π stacking interactions. The resulting C2′-iodinated azanucleoside products serve as key intermediates for further functionalization into diverse azanucleoside analogues. The utility of this method is demonstrated by a concise synthesis of forodesine ($\beta : \alpha > 20 : 1$, 8 steps, 20% overall yield). To our knowledge, few existing methods achieve such stereocontrol using solely achiral molecules in the absence of chiral catalysts, particularly in nucleoside synthesis. This work not only expands fundamental chemical understanding but also provides access to underexplored azanucleosides for therapeutic development.

Author contributions

F. C. and H. W. conceived the idea and guided the project. H. W. wrote the manuscript with feedback from the other authors. Y. Z. made the initial observations and analyzed the results. Y. Z., M. L., K. Z., J. M., S. G. and P. T. explored substrate scope and performed derivatizations. J. Z. and Y. L. performed the density functional theory calculations on the reaction mechanism.

Conflicts of interest

A patent application (grant no. 202411109085.7, China) dealing with the synthesis of forodesine has been applied, and Huijing Wang and Fener Chen may benefit from royalty payments.

Data availability

CCDC 2378539 contains the supplementary crystallographic data for this paper.[69]

Additional data supporting the findings described in this paper are available in the supplementary information (SI) and available from the corresponding author upon reasonable request. Supplementary information: detailed experimental procedures, compound characterization data (including NMR spectra and HPLC chromatograms), and additional computational results. Supplementary information is available. See DOI: https://doi.org/10.1039/d5sc08431h.

Acknowledgements

We are grateful for the financial support from the National Natural Science Foundation of China (Grant No. 22201192, U24A20482, and 22301228).

Notes and references

1 M. Guinan, C. Benckendorff, M. Smith and G. J. Miller, Recent advances in the chemical synthesis and evaluation of anticancer nucleoside analogues, *Molecules*, 2020, **25**, 2050.
2 G. Li, T. Yue, P. Zhang, W. Gu, L. J. Gao and L. Tan, Drug discovery of nucleos(t)ide antiviral agents: dedicated to Prof. Dr. Erik De Clercq on occasion of his 80th birthday, *Molecules*, 2021, **26**, 923.
3 M. I. Elzagheid, Nucleosides and nucleoside analogues as emerging antiviral drugs, *Mini-Rev. Org. Chem.*, 2021, **18**, 672–679.

4 S. Man, Y. Lu, L. Yin, X. Cheng and L. Ma, Potential and promising anticancer drugs from adenosine and its analogs, *Drug Discov. Today*, 2021, **26**, 1490–1500.
5 Q. Wang, K. Chen, Y. Wang, Z. Rao and X. Zhang, Biotechnological synthesis of nucleoside analogs: recent progress and perspectives, *Green Synth. Catal.*, 2025, DOI: 10.1016/j.gresc.2025.05.002.
6 P. Merino, T. Tejero and I. Delso, Current developments in the synthesis and biological activity of aza-C-nucleosides: immucillins and related compounds, *Curr. Med. Chem.*, 2008, **15**, 954–967.
7 G. B. Evans, P. C. Tyler and V. L. Schramm, Immucillins in infectious diseases, *ACS Infect. Dis.*, 2018, **4**, 107–117.
8 G. B. Evans, V. L. Schramm and P. C. Tyler, The immucillins: design, synthesis and application of transition- state analogues, *Curr. Med. Chem.*, 2015, **22**, 3897–3909.
9 R. W. Miles, P. C. Tyler, R. H. Furneaux, C. K. Bagdassarian and V. L. Schramm, One-third-the-sites transition-state inhibitors for purine nucleoside phosphorylase, *Biochemistry*, 1998, **37**, 8615–8621.
10 G. A. Kicska, L. Long, H. Hörig, C. Fairchild, P. C. Tyler, R. H. Furneaux, V. L. Schramm, H. L. Kaufman and H. Immucillin, a powerful transition-state analog inhibitor of purine nucleoside phosphorylase, selectively inhibits human T lymphocytes, *Proc. Natl. Acad. Sci. U. S. A.*, 2001, **98**, 4593–4598.
11 S. Bantia, P. J. Miller, C. D. Parker, S. L. Ananth, L. L. Horn, J. M. Kilpatrick, P. E. Morris, T. L. Hutchison, J. A. Montgomery and J. S. Sandhu, Purine nucleoside phosphorylase inhibitor BCX-1777 (Immucillin-H) a novel potent and orally active immunosuppressive agent, *Int. Immunopharmacol.*, 2001, **1**, 1199–1210.
12 A. Korycka, J. Z. Błoński and T. Robak, Forodesine (BCX-1777, Immucillin H) – a new purine nucleoside analogue: mechanism of action and potential clinical application, *Mini Rev. Med. Chem.*, 2007, **7**, 976–983.
13 T. K. Warren, J. Wells, R. G. Panchal, K. S. Stuthman, N. L. Garza, S. A. V. Tongeren, L. Dong, C. J. Retterer, B. P. Eaton, G. Pegoraro, S. Honnold, S. Bantia, P. Kotian, X. Chen, B. R. Taubenheim, L. S. Welch, D. M. Minning, Y. S. Babu, W. P. Sheridan and S. Bavari, Protection against filovirus diseases by a novel broad-spectrum nucleoside analogue BCX4430, *Nature*, 2014, **508**, 402–405.
14 J. G. Julander, S. Bantia, B. R. Taubenheim, D. M. Minning, P. Kotian, J. D. Morrey, D. F. Smee, W. P. Sheridan and Y. S. Babu, BCX4430, a novel nucleoside analog, effectively treats yellow fever in a Hamster model, *Antimicrob. Agents Chemother.*, 2014, **53**, 6607–6614.
15 E. De Clercq, C-nucleosides to be revisited, *J. Med. Chem.*, 2016, **59**, 2301–2311.
16 R. Taylor, P. Kotian, T. Warren, R. Panchal, S. Bavari, J. Julander, S. Dobo, A. Rose, Y. El-Kattan, B. Taubenheim, Y. Babu and W. P. Sheridan, BCX4430 – a broad-spectrum antiviral adenosine nucleoside analog under development for the treatment of Ebola virus disease, *J. Infect. Public Health*, 2016, **9**, 220–226.
17 J. G. Julander, V. Siddharthan, J. Evans, R. Taylor, K. Tolbert, C. Apuli, J. Stewart, P. Collins, M. Gebre, S. Neilson, A. Van Wettere, Y. M. Lee, W. P. Sheridan, J. D. Morrey and Y. S. Babu, Efficacy of the broad-spectrum antiviral compound BCX4430 against Zika virus in cell culture and in a mouse model, *Antiviral Res.*, 2017, **137**, 14–22.
18 J. B. Westover, A. Mathis, R. Taylor, L. Wandersee, K. W. Bailey, E. J. Sefing, B. T. Hickerson, K. H. Jung, W. P. Sheridan and B. B. Gowen, *Antiviral Res.*, 2018, **156**, 38–45.
19 J. G. Julander, J. F. Demarest, R. Taylor, B. B. Gowen, D. M. Walling, A. Mathis and Y. S. Babu, An update on the progress of galidesivir (BCX4430), a broad-spectrum antiviral, *Antiviral Res.*, 2021, **195**, 105180.
20 Y. Xie, L. Y. Chi, S. Q. Liu and W. Y. Zhu, BCX4430 inhibits the replication of rabies virus by suppressing mTOR-dependent autophagy *in vitro*, *Virology*, 2023, **585**, 21–31.
21 K. J. Sparrow, R. Shrestha, J. M. Wood, K. Clinch, B. L. Hurst, H. Wang, B. B. Gowen, J. G. Julander, E. B. Tarbet, A. M. McSweeney, V. K. Ward, G. B. Evans and L. D. Harris, An Isomer of galidesivir that potently inhibits influenza viruses and members of the bunyavirales order, *ACS Med. Chem. Lett.*, 2023, **14**, 506–513.
22 Y. S. Babu, P. L. Kotian, S. Bantia, M. Wu, V. S. Kumar, *Preparation of antiviral aza-sugar-containing nucleosides*, WO 2014078778, 2014.
23 Y. S. Babu, P. L. Kotian, S. Bantia, M. Wu and V. S. Kumar, Antiviral azasugar-containing nucleosides, *US Pat.*, US20150291596, 2015.
24 G. Ni, Y. Du, F. Tang, J. Liu, H. Zhao and Q. Chen, Review of α-nucleosides: from discovery, synthesis to properties and potential applications, *RSC Adv.*, 2019, **9**, 14302–14320.
25 J. Bouton, S. Van Calenbergh and J. Hullaert, Sydnone ribosides as a platform for the synthesis of pyrazole C-nucleosides: a unified synthesis of Formycin B and Pyrazofurin, *Org. Lett.*, 2020, **22**, 9287–9291.
26 Q. Li, E. Lescrinier, E. Groaz, L. Persoons, D. Daelemans, P. Herdewijn and S. De Jonghe, Synthesis and biological evaluation of pyrrolo[2,1-*f*][1,2,4]triazine C-nucleosides with a ribose, 2'-deoxyribose, and 2',3'-dideoxyribose sugar moiety, *ChemMedChem*, 2018, **13**, 97–104.
27 T. Liu, Z. Zhu, H. Ren, Y. Chen, G. Chen, M. Cheng, D. Zhao, J. Shen, W. Zhu, B. Xiong and Y. L. Chen, Efficient syntheses of alpha- and beta-C-nucleosides and the origin of anomeric selectivity, *Org. Chem. Front.*, 2018, **5**, 1992–1999.
28 P. Nie, E. Groaz, D. Daelemans and P. Herdewijn, Xylo-C-Nucleosides with a pyrrolo[2,1-f][1,2,4]triazin-4-amine heterocyclic base: synthesis and antiproliferative properties, *Bioorg. Med. Chem. Lett.*, 2019, **29**, 1450–1453.
29 P. Nie, E. Groaz and P. Herdewijn, Synthesis of a threosyl-C-nucleoside phosphonate, *Eur. J. Org Chem.*, 2019, **2019**, 6666–6672.
30 H. Marzag, M. Zerhouni, H. Tachallait, L. Demange, G. Robert, K. Bougrin, P. Auberger and R. Benhida, Modular synthesis of new C-aryl-nucleosides and their anti-CML activity, *Bioorg. Med. Chem. Lett.*, 2018, **28**, 1931–1936.

31 H. Tachallait, M. Safir Filho, H. Marzag, K. Bougrin, L. Demange, A. R. Martin and R. Benhida, A Straightforward and versatile $FeCl_3$ catalyzed Friedel-Crafts C -glycosylation process. Application to the synthesis of new functionalized C -nucleosides, *New J. Chem.*, 2019, **43**, 5551–5558.
32 H. Gong and M. R. Gagné, Diastereoselective Ni-catalyzed Negishi cross-coupling approach to saturated, fully oxygenated *C*-alkyl and *C*-aryl glycosides, *J. Am. Chem. Soc.*, 2008, **130**, 12177–12183.
33 Q. Wang, S. An, Z. Deng, W. Zhu, Z. Huang, G. He and G. Chen, Palladium-catalysed C–H glycosylation for synthesis of C-aryl glycosides, *Nat. Catal.*, 2019, **2**, 793–800.
34 Y. Li, Z. Wang, L. Li, X. Tian, F. Shao and C. Li, Chemoselective and diastereoselective synthesis of C-Aryl nucleoside analogues by Nickel-catalyzed cross-coupling of furanosyl acetates with aryl iodides, *Angew. Chem., Int. Ed.*, 2022, **61**, e202110391.
35 R. Xie, J. Xu, H. Shi, C. Xiao, N. Wang, N. Huang and H. Yao, Stereocontrolled Synthesis of aryl C-nucleosides under ambient conditions, *Org. Lett.*, 2024, **26**, 5162–5166.
36 S. O. Badir, A. Dumoulin, J. K. Matsui and G. A. Molander, Synthesis of reversed C-acyl glycosides through Ni/photoredoxdual catalysis, *Angew. Chem., Int. Ed.*, 2018, **57**, 6610–6613.
37 A. Dumoulin, J. K. Matsui, Á. Gutiérrez-Bonet and G. A. Molander, Synthesis of non-classical arylated C-saccharides through Nickel/photoredox dual catalysis, *Angew. Chem., Int. Ed.*, 2018, **57**, 6614–6618.
38 Y. Ma, S. Liu, Y. Xi, H. Li, K. Yang, Z. Cheng, W. Wang and Y. Zhang, Highly stereoselective synthesis of aryl/heteroaryl-C-nucleosides via the merger of photoredox and Nickel catalysis, *Chem. Commun.*, 2019, **55**, 14657–14660.
39 Q. Wang, J. Duan, P. Tang, G. Chen and G. He, Synthesis of non-classical heteroaryl C-glycosides via Minisci-type alkylation of N-heteroarenes with 4-glycosyl-dihydropyridines, *Sci. China Chem.*, 2020, **63**, 1613–1618.
40 Y. Wei, B. Ben-zvi and T. Diao, Diastereoselective synthesis of aryl C-glycosides from glycosyl esters via C–O bond homolysis, *Angew. Chem., Int. Ed.*, 2021, **6**, 9433–9438.
41 G. B. Evans, R. H. Furneaux, G. J. Gainsford, V. L. Schramm and P. C. Tyler, Synthesis of transition state analogue inhibitors for purine nucleoside phosphorylase and N-riboside hydrolases, *Tetrahedron Lett.*, 2000, **56**, 3053–3062.
42 G. B. Evans, R. H. Furneaux, T. L. Hutchison, H. S. Kezar, P. E. Morris, V. L. Schramm and P. C. Tyler, Addition of lithiated 9-deazapurine derivatives to a carbohydrate cyclic imine: convergent synthesis of the aza- C -nucleoside immucillins, *J. Org. Chem.*, 2001, **66**, 5723–5730.
43 V. P. Kamath, J. Xue, J. J. Juarez-Brambila and P. E. Morris, Alternative route towards the convergent synthesis of a human purine nucleoside phosphorylase inhibitor – forodesine HCl, *Tetrahedron Lett.*, 2009, **50**, 5198–5200.
44 V. P. Kamath, J. Xue and J. J. Juarez-Brambila, Synthesis of analogs of forodesine HCl, a human purine nucleoside phosphorylase inhibitor – Part II, *Bioorg. Med. Chem. Lett.*, 2009, **19**, 2627–2629.
45 M. Zhang, F. Xue, J. Ou, Y. Huang, F. Lu, B. Zhou, Z. Zheng, X. Y. Liu, W. Zhong and Y. Qin, Practical synthesis of immucillins BCX-1777 and BCX-4430, *Org. Chem. Front.*, 2020, **7**, 3675–3680.
46 J. Ou, M. Zhang, P. Li, F. Xue and Y. Qin, Synthesis of purine nucleoside phosphorylase inhibitor Forodesine, *West China J. Pharm. Sci.*, 2021, **36**, 495–500.
47 K. A. Krishnakumar and R. S. Lankalapalli, Synthesis of immucillins BCX-1777 and BCX-4430 from a common precursor, *Eur. J. Org Chem.*, 2022, e202200428.
48 S. E. Denmark, W. E. Kuester and M. T. Burk, Catalytic, asymmetric halofunctionalization of alkenes-a critical perspective, *Angew. Chem., Int. Ed.*, 2012, **51**, 10938–10953.
49 R. Kristianslund, J. E. Tungen and T. V. Hansen, Catalytic enantioselective iodolactonization reactions, *Org. Biomol. Chem.*, 2019, **17**, 3079–3092.
50 S. Liu, B. Zhang, W. Xiao, Y. Li and J. Deng, Recent advances in catalytic asymmetric syntheses of functionalized heterocycles *via* halogenation/chalcogenation of carbon-carbon unsaturated bonds, *Adv. Synth. Catal.*, 2022, **364**, 3974–4005.
51 J. Yan, Z. Zhou, Q. He, G. Chen, H. Wei and W. Xie, The applications of catalytic asymmetric halocyclization in natural product synthesis, *Org. Chem. Front.*, 2022, **9**, 499–516.
52 Q. Wang, J. Mu, J. Zeng, L. Wan, Y. Zhong, Q. Li, Y. Li, H. Wang and F. Chen, Additive-controlled asymmetric iodocyclization enables enantioselective access to both α- and β-nucleosides, *Nat. Commun.*, 2023, **14**, 138.
53 R. A. Sheldon, The E factor 25 years on: the rise of green chemistry and sustainability, *Green Chem.*, 2017, **19**, 18–43.
54 A. Antenucci and S. Dughera, Usefulness of the global E factor as a tool to compare different catalytic strategies: four case studies, *Catalysts*, 2023, **13**, 102.
55 K. Maruoka and T. Ooi, Enantioselective amino acid synthesis by chiral phase-transfer catalysis, *Chem. Rev.*, 2003, **103**, 3013–3028.
56 T. Ooi and K. Maruoka, Recent advances in asymmetric phase-transfer catalysis, *Angew. Chem., Int. Ed.*, 2007, **46**, 4222–4266.
57 S. Jew and H. Park, Cinchona-based phase-transfer catalysts for asymmetric synthesis, *Chem. Commun.*, 2009, **46**, 7090–7103.
58 S. Shirakawa and K. Maruoka, Recent developments in asymmetric phase-transfer reactions, *Angew. Chem., Int. Ed.*, 2013, **52**, 4312–4348.
59 H. J. Lee and K. Maruoka, Recent asymmetric phase-transfer catalysis with chiral binaphthyl-modified and related phase-transfer catalysts over the last 10 years, *Chem. Rec.*, 2023, **23**, e202200286.
60 H. J. Lee and K. Maruoka, Asymmetric phase-transfer catalysis, *Nat. Rev. Chem.*, 2024, **8**, 851–869.
61 P. Pecchini, M. Fochi, F. Bartoccini, G. Piersanti and L. Bernardi, Enantioselective organocatalytic strategies to access noncanonical α-amino acids, *Chem. Sci.*, 2024, **15**, 5832–5868.

62 E. J. Corey, F. Xu and M. C. Noe, Rational approach to catalytic enantioselective enolate alkylation using a structurally rigidified and defined chiral quaternary ammonium salt under phase transfer conditions, *J. Am. Chem. Soc.*, 1997, **119**, 12414–12415.

63 S. Woo, Y. G. Kim, B. Lim, J. Oh, Y. Lee, H. Gwon and K. Nahm, An unusual electronic effect of an aromatic-F in phase-transfer catalysts derived from cinchona-alkaloid, *Org. Lett.*, 2002, **4**, 4245–4248.

64 S. Woo, Y. G. Kim, B. Lim, J. Oh, Y. Lee, H. Gwon and K. Nahm, Dimeric cinchona ammonium salts with benzophenone linkers: enantioselective phase transfer catalysts for the synthesis of α-amino acids, *RSC Adv.*, 2018, **8**, 2157–2160.

65 J. Oh, J. Park and K. Nahm, Counter-rotatable dual cinchona quinuclidinium salts and their phase transfer catalysis in enantioselective alkylation of glycine imines, *Chem. Commun.*, 2021, **57**, 6816–6819.

66 J. P. Perdew, K. Burke and M. Ernzerhof, Generalized Gradient Approximation Made Simple, *Phys. Rev. Lett.*, 1997, **78**, 1396.

67 T. Lu and Q. Chen, Interaction region indicator: a simple real space function clearly revealing both chemical bonds and weak interactions, *Chem.: Methods*, 2021, **1**, 231–239.

68 T. Lu and F. Chen, Multiwfn: a multifunctional wavefunction analyzer, *J. Comput. Chem.*, 2012, **33**, 580–585.

69 CCDC 2378539: Experimental Crystal Structure Determination, 2025, DOI: 10.5517/ccdc.csd.cc2kv22l.